HHS Public Access

Author manuscript

Nat Med. Author manuscript; available in PMC 2018 February 01.

Published in final edited form as:

Nat Med. 2017 August ; 23(8): 938–944. doi:10.1038/nm.4373.

Resolution of inflammation by interleukin-9-producing type 2 innate lymphoid cells

Simon Rauber[1], **Markus Luber**[1], **Stefanie Weber**[1], **Lisa Maul**[1], **Alina Soare**[1], **Thomas Wohlfahrt**[1], **Neng-Yu Lin**[1], **Katharina Dietel**[1], **Aline Bozec**[1], **Martin Herrmann**[1], **Mark H. Kaplan**[2], **Benno Weigmann**[3], **Mario M. Zaiss**[1], **Ursula Fearon**[4], **Douglas J. Veale**[5], **Juan D. Canete**[6], **Oliver Distler**[7], **Felice Rivellese**[8], **Costantino Pitzalis**[8], **Markus F. Neurath**[3], **Andrew N.J. McKenzie**[9], **Stefan Wirtz**[3], **Georg Schett**[1], **Jörg H.W. Distler**[1], and **Andreas Ramming**[1]

[1]Department of Internal Medicine 3 – Rheumatology and Immunology, Friedrich-Alexander-University Erlangen-Nürnberg (FAU) and Universitätsklinikum Erlangen, Erlangen, Germany [2]Herman B Wells Center for Pediatric Research, Indianapolis, USA [3]Department of Internal Medicine 1, Friedrich-Alexander-University Erlangen-Nürnberg (FAU) and Universitätsklinikum Erlangen, Erlangen, Germany [4]Molecular Rheumatology, School of Medicine, Trinity Biomedical Sciences Institute, Trinity College Dublin, Dublin, Ireland [5]Centre for Arthritis and Rheumatic Diseases, St. Vincent's University Hospital, Dublin, Ireland [6]Departamento de Reumatología, Hospital Clínic de Barcelona e IDIBAPS, Barcelona, Spain [7]Division of Rheumatology, University Hospital Zurich, Zurich, Switzerland [8]Centre for Experimental Medicine and Rheumatology, William Harvey Research Institute, Barts and the London School of Medicine and Dentistry, Queen Mary University of London and Barts Health NHS Trust, London, UK [9]MRC Laboratory of Molecular Biology, Cambridge, UK

Abstract

Inflammatory diseases such as arthritis are chronic conditions that fail to resolve spontaneously. While the cytokine and cellular pathways triggering arthritis are well defined, those responsible for the resolution of inflammation are incompletely characterized. Here we identified IL-9-producing type 2 innate lymphoid cells (ILC2s) as a molecular and cellular pathway that orchestrates the resolution of chronic inflammation. In mice, the absence of IL-9 impaired ILC2 proliferation, activation of regulatory T cells (T_{reg}) and resulted in chronic arthritis with excessive cartilage destruction and bone loss. In contrast, treatment with IL-9 promoted ILC2-dependent

Corresponding author: Andreas Ramming, Department of Internal Medicine 3, Rheumatology and Immunology, University of Erlangen-Nürnberg, Ulmenweg 18, 91054 Erlangen, Germany. Phone: +49-9131-8543048. Fax: +49-9131-8536448. andreas.ramming@uk-erlangen.de.

Competing financial interests

The authors declare no competing financial interests.

Author Contributions

Design of the study: S.R., G.S., J.H.W.D., A.R.

Acquisition of data: S.R., M.L., S.We., L.M., A.S., T.W., N.-Y.L., K.D., M.G., A.R.

Interpretation of data: S.R., A.B., M.H., A.N.J.M., B.W., M.M.Z., U.F., D.J.V., J.D.C., O.D., F.R., C.P., S.W., M.F.N., G.S., J.H.W.D., A.R.

Support of material: A.B., M.H., M.H.K., B.W., U.F., D.J.V., J.D.C., O.D., F.R., C.P., M.F.N., A.N.J.M., S.W.

Manuscript preparation: S.R., G.S., J.H.W.D., A.R.

T_{reg} activation and effectively induced resolution of inflammation and protection of bone. Rheumatoid arthritis patients in remission demonstrated high numbers of IL-9$^+$ ILC2s in the joints and in the circulation. Hence, fostering IL-9-mediated ILC2 activation may offer a novel therapeutic approach inducing resolution of inflammation rather than suppression of inflammatory responses.

Keywords

Resolution of inflammation; chronic inflammation; IL-9; innate lymphoid cells; arthritis; bone loss

Introduction

Resolution of inflammation is still incompletely understood. In chronic inflammatory diseases the physiological process of resolution of inflammation is impaired [1,2]. Diseases such as rheumatoid arthritis (RA) often start in young adulthood, but fail to wane requiring life-long immunosuppressive treatment[3]. Furthermore, the body's failure to effectively terminate inflammation leads to pronounced tissue damage such as bone loss[4,5]. Current treatment strategies for chronic inflammatory diseases like RA target pro-inflammatory cytokines and hence the activation process of inflammation rather than promoting its resolution[6,7]. While lipid mediators such as resolvins have been implicated in resolution of inflammation[8], cytokine pathways for governing this process are largely undefined to date. Identification of such pathways, however, would allow rebalancing of inflammatory responses rather than generally suppressing inflammation and may substantially add to the development of new treatment possibilities. We were therefore interested in identifying novel pathways governing the resolution of arthritis. We identified interleukin (IL)-9 as a master regulator for resolution of arthritis and found that type 2 innate lymphoid cells (ILC2s), which produce IL-9 are essential for the initiation of this resolution process.

Results

Antigen-induced arthritis (AIA) is a standard model of arthritis with spontaneous resolution (Supplementary Fig. 1a)[9,10]. In contrast, we observed that the course of AIA in *Il9*$^{-/-}$ mice was highly chronic (Fig. 1a). While joint swelling resolved spontaneously within 12–16 days in WT mice, it persisted beyond 42 days without signs of resolution in *Il9*$^{-/-}$ mice. The chronic inflammatory phenotype of *Il9*$^{-/-}$ mice was rescued by overexpression of IL-9 via hydrodynamic gene transfer (HDGT), using mini-circle (MC) vectors encoding IL-9 (*Il9* MC) (Fig. 1b). Histological analysis of the affected knee joints of *Il9*$^{-/-}$ mice at d42 confirmed persistent synovitis and demonstrated excessive degradation of cartilage and bone and higher numbers of osteoclasts in *Il9*$^{-/-}$ compared to WT mice (Fig. 1c–e). Microcomputed tomography showed a pronounced loss of the trabecular network and bone volume as signs of inflammation-induced osteopenia in *Il9*$^{-/-}$ mice (Fig. 1f). In contrast to AIA, absence of IL-9 did not affect the course of acute inflammatory arthritis induced by monosodium urate crystal, which exclusively relies on neutrophil activation (Supplementary Fig. 1b).

Mice expressing the transgenic T cell receptor (TCR) KRN and the MHC class II allele A^{g7} (K/BxN mice) develop autoantibodies against glucose-6-phosphate isomerase[11]. Passive transfer of serum from those mice is commonly used to initiate chronic arthritis (SIA)[12] with inflammation persisting over several weeks. To assess the therapeutic potential of IL-9 to promote its resolution, we overexpressed IL-9 using HDGT during the effector phase of SIA (3 days after induction of SIA). Consistent with our previous findings in AIA, overexpression of IL-9 did not have major effects on the initiation phase of SIA or on the maximal intensity of arthritis, but strongly accelerated its resolution (Fig. 2a). Joint swelling completely resolved within 9 days in mice with forced expression of IL-9, whereas arthritis in mice injected with the control vector was still worsening at day 9 (Fig. 2a, b). Histological analysis at day 9 showed substantially less synovitis in the paws of mice injected with *Il9* MC (Fig. 2b, c). Accelerated resolution of arthritis by IL-9 translated into reduced tissue damage with preservation of cartilage integrity, reduced osteoclast counts and decreased bone erosions (Fig. 2b–e).

To further characterize the mechanism by which IL-9 fosters the resolution of arthritis, the kinetics of pro- and anti-inflammatory mediators were analyzed in the serum and joints of arthritic *Il9*$^{-/-}$ and WT mice (Fig. 3a, Supplementary. Fig. 2a, b). Time kinetics and concentrations of most key cytokine mediators such as tumor necrosis factor α (TNF-α), IL-6, interferon (IFN)-γ, IL-2 and IL-4 did not significantly differ between WT and *Il9*$^{-/-}$ mice. However, pronounced differences in IL-17 levels were observed which remained persistently high in *Il9*$^{-/-}$ AIA mice, but returned to baseline levels in WT AIA mice. The selective upregulation of IL-17 was associated with enhanced Th17 polarization particularly in inflamed joints of *Il9*$^{-/-}$ mice, whereas naïve, memory and effector T cell counts were comparable in WT and *Il9*$^{-/-}$ mice (Fig. 3b, c). These data demonstrate a shift to a persistent Th17-cell-driven immune response in *Il9*$^{-/-}$ mice. To address the possibility that IL-9 serves as an intrinsic regulator of Th17 differentiation, CD4 T cells from WT and *Il9*$^{-/-}$ mice were stimulated under Th17-inducing conditions. Differentiation into conventional as well as into inflammatory Th17 cells was comparable in WT and *Il9*$^{-/-}$ mice (Fig. 3d) providing no evidence for an intrinsic defect in Th17 development in *Il9*$^{-/-}$ mice but arguing for a central role of other cell types for the IL-9-induced inhibition of Th17 polarization.

To identify these target cells of IL-9, we next analyzed regulatory T cells (T_{regs}) in WT and *Il9*$^{-/-}$ mice at day 42 after immunization, when inflammation was resolved in WT mice, but still persisted in *Il9*$^{-/-}$ mice. Total numbers of $CD4^{pos}CD25^{pos}Foxp3^{pos}$ T_{regs} were comparable in *Il9*$^{-/-}$ compared to WT mice (Fig. 3e). However, the suppressive capacity of T_{regs} from *Il9*$^{-/-}$ mice was significantly decreased as shown by co-culture of CFSE-labeled $CD25^{neg}Foxp3^{neg}$ effector T cells (T_{effs}) with $Foxp3^{pos}$ T_{regs} and subsequent analyses of proliferation of T_{effs} (Fig. 3f). The functional defect of *Il9*$^{-/-}$ T_{regs} was associated with significantly decreased expression levels of functionally important effector molecules[13,14] such as GITR and ICOS in *Il9*$^{-/-}$ T_{regs} (Fig. 3g). To exclude the possibility that effector T cells from *Il9*$^{-/-}$ mice are resistant to the effects of T_{regs}, the susceptibility of *Il9*$^{-/-}$ and WT effector T cells to the suppressive effects of WT T_{regs} was assessed. Both, proliferation and cytokine production did not differ between *Il9*$^{-/-}$ and WT responder T cells (Fig. 3h, i).

In line with previous reports, exogenous IL-9 modestly enhanced T_{reg} function *in vitro* (data not shown)[15]. However, prestimulation of T_{regs} from *Il9*$^{-/-}$ mice with IL-9 and adoptive transfer of these cells into *Il9*$^{-/-}$ mice did not prevent chronification of AIA (Supplementary Fig. 3a). We therefore further aimed to define cellular intermediates that might be involved in IL-9-induced resolution of inflammation. To explore the source of IL-9 in arthritis, AIA was induced in *Il9*^{citrine} reporter mice[16]. The majority of IL-9-producing cells did not express lineage (Lin) specific markers that define Lin^{pos} lymphocytic and myeloid populations including potential IL-9-producing cell types such as Th9 cells[17–20] and mast cells[21] (Fig. 4a). More than 80% of the Lin^{neg} citrine^{pos} cells expressed ST2, ICOS (Fig. 4a), CD25, CD90, and Sca-1 (Supplementary Fig. 3b) suggesting that innate lymphoid cells type 2 (ILC2) are the predominant source of IL-9 during the resolution phase of arthritis, as defined as the segment of time between the peak of inflammation and 50% regression[22] (Fig. 4a). These data were supported by quantitative analysis of synovial tissue sections from AIA WT mice stained with immunofluorescence labeled antibodies. ILC2s were identified as the major source of IL-9 during resolution of AIA (Supplementary Fig. 3c). Furthermore, expression levels of mast cell-specific genes in inflamed joints did not differ between WT and *Il9*$^{-/-}$ mice (Supplementary Fig. 3d, e). ILC2 numbers were profoundly decreased in the synovium of *Il9*$^{-/-}$ mice (Fig. 4b). Impaired proliferation may account for the reduced numbers of ILC2s, as the number of proliferating Ki67 positive ILC2s was significantly decreased in arthritic knee joints of *Il9*$^{-/-}$ mice (Fig. 4b). In line with previous reports that IL-9 production by ILC2 acts in an autocrine loop to promote ILC proliferation[23,24], induction of ILC2s by overexpression of IL-25 and IL-33 using HDGT confirmed an intrinsic defect of ILC2 proliferation in *Il9*$^{-/-}$ mice (Supplementary Fig. 4a). Addition of IL-9 led to complete reconstitution of ILC2s. To confirm the relevance of this finding for the pathogenesis of chronic arthritis, multicolor immunofluorescence microscopy (IF) revealed that IL-9-producing ILC2s are located in close proximity to CD3^{pos}Foxp3^{pos} T_{regs} in the inflamed synovium (Fig. 4c). The co-localization of ILC2s and T_{regs} in the inflamed tissue supports cellular interactions that might be of functional relevance for T_{reg} suppression. Indeed, stimulation of ILC2s with IL-9 induced upregulation of the T_{reg}-receptor-associated ligands GITRL and ICOSL (Fig. 4d).

To determine the functional impact of interactions between ILC2s and T_{regs}, we performed T_{reg} suppression assays in the presence and absence of ILC2s. These assays demonstrated that ILC2s stimulated the suppressive capacity of T_{regs}. Whereas *Il9*$^{-/-}$ T_{regs} alone did not suppress T_{effs} proliferation, addition of ILC2s completely rescued this impaired suppressive capacity of *Il9*$^{-/-}$ T_{regs} (Fig. 4e). Transwell experiments revealed that these ILC2-mediated effects on *Il9*$^{-/-}$ T_{regs} required direct cell contacts (Supplementary Fig. 4b). Screening for potential mediators of this contact dependent effect revealed that ILC2s express high levels of GITRL and ICOSL, which are known to promote the suppressive capacity of Tregs[13,14]. Blockade of GITR/GITRL and ICOS/ICOSL reversed the ILC2 mediated effects on the suppressive capacity of *Il9*$^{-/-}$ T_{regs} (Fig. 4e). Consistent with this model, ligand binding to GITR and ICOS in *Il9*$^{-/-}$ T_{regs} also restored the suppressive capacity of *Il9*$^{-/-}$ T_{regs} in the absence of ICOSL/GITRL-bearing ILC2s (Fig. 4f). *In vivo*, adoptive transfer of *Il9*$^{-/-}$ T_{regs}, which had been pre-activated via GITR and ICOS *ex vivo*, led to a regain of their suppressive activity in the AIA model (Fig. 4g), highlighting that receptor/ligand specific

interactions between ILC2s and T_{regs} activate the suppressive capacity of T_{regs}. In order to confirm the functional impact of ILC2s on the resolution of inflammation, ILC2s were adoptively transferred into *Il9*$^{-/-}$ mice with AIA. Adoptive transfer of ILC2s inhibited activation of Th17 cells and promoted resolution of inflammation in *Il9*$^{-/-}$ mice (Fig. 4h, Supplementary Fig. 4c).

To investigate the role of IL-9 for the resolution of inflammation in humans, synovial tissues of patients with RA as prototypical chronic inflammatory joint disease were analyzed. In line with previous reports[25,26], the dominant part of IL-9 expression in the synovial membranes of active RA patients came from Lin^{pos} cells (Fig. 5a, b). Only low numbers of IL-9^{pos} ILC2s were found in active RA despite extensive synovial inflammation. In contrast, RA patients in clinical remission exhibited high numbers of Lin^{neg} IL-9^{pos} ILC2s and a significant decline of Lin^{pos} IL-9^{pos} cells (Fig. 5a, b). Patients with acute joint inflammation after trauma demonstrated only a tendency towards increased numbers of Lin^{pos} IL-9^{pos} and Lin^{neg} IL-9^{pos} cells compared to healthy individuals. Longitudinal analysis of infiltrates in synovial tissue of RA patients before and 6 months after start of anti-inflammatory treatment showed a shift in the cellular source of IL-9 from Lin^{pos} IL-9^{pos} cells during active disease to Lin^{neg} IL-9^{pos} ILC2s 6 months later when anti-rheumatic drugs had led to remission of arthritis (Fig. 5c). Stratification of RA patients according to disease activity revealed that ILC2 numbers in the blood were particularly low in RA patients with persistent inflammatory activity, but significantly higher in RA patients that were in disease remission (Fig. 5d, e). ILC2 numbers significantly correlated with disease activity in RA as measured by standardized disease activity score 28 (DAS28) (Fig. 5e). Longitudinal observations of patients revealed a reciprocal link between ILC2s and disease activity (Fig. 5f). These data, taken in combination with the results from the mouse models, indicate a pivotal role of ILC2s in the resolution of chronic inflammation and prevention of immunochronicity.

Discussion

Our data demonstrate that IL-9 fosters resolution of inflammation and prevents the chronification of arthritis. IL-9 virtually exclusively affected the resolution phase of the disease, while only minor effects were observed in the induction phase. In some experiments a tendency to higher peak inflammation was observed in IL-9 deficient mice although these effects were only mild and not consistent among the experiments. These observations may be explained by the regulatory action of IL-9 starting already before the peak of inflammation has been reached. Nonetheless induction of resolution of arthritis clearly came up as the primary action of IL-9 in arthritis contrasting the effects of other known cytokines involved in arhritis such as TNFα, IL-6 and IL-17, which are primarily involved in the induction phase and which are successfully targeted by modern cytokine inhibitors. Our data show that resolution of arthritis is mechanistically based on the induction of ILC2s by IL-9, which in turn elicits GITR/GITRL and ICOS/ICOSL dependent activation of T_{regs}. This IL-9-mediated forced resolution of arthritis translates into reduced tissue damage such as bone and cartilage loss, which usually result from chronic inflammation in the context of arthritis. Our data provide evidence that IL-9 has a dichotomous function in different phases of inflammation. Previous studies have shown that under certain circumstances IL-9 can promote inflammation in acute models[15,16,27–28]. In chronic arthritis however, IL-9 acts as a

cytokine governing the resolution phase of the disease. These findings are remarkable as resolution of inflammation is preferentially attributed to lipid mediators such as resolvins to date and little was known about innate/adaptive immune system interactions in orchestrating the resolution process[2]. IL-9 and the function of ILC2s in this process provide strong support for the existence of immune pathways, which primarily foster the resolution of inflammation and restore immune homeostasis in chronic inflammatory diseases. From the therapeutic perspective such approaches are highly attractive as they provide an anchor for allowing re-balancing of the pathologic inflammatory response in the near future rather than exposing patients to a broad suppression of inflammatory responses.

Supplementary Material

Refer to Web version on PubMed Central for supplementary material.

Acknowledgments

The authors thank to Mónica Pascual, Katja Dreissigacker, Regina Kleinlein, Maria Comazzi, Daniela Weidner and Barbara Happich for excellent technical assistance. We thank Uwe Appelt and Markus Mroz of the Core Unit Cell Sorting and Immunomonitoring Erlangen for cell sorting. This work was supported by the Deutsche Forschungsgemeinschaft (RA 2506/3-1, RA 2506/4-1 to A.R.; DI 1537/5-1, DI 1537/7-1, DI 1537/8-1, DI 1537/9-1, DI 1537/11-1 to J.H.W.D.; SCHE 1583/7-1 to G.S.; SPP1468-IMMUNOBONE and CRC1181 to G.S. and J.H.W.D.), the Bundesministerium für Bildung und Forschung (METHARTHROS to G.S. and J.H.W.D.), the Marie Curie project OSTEOIMMUNE (to G.S. and J.H.W.D.), the TEAM project of the European Union and the IMI funded project RTCure (to G.S.), Else Kröner-Fresenius-Stiftung 2014_A184 (to A.R.), the Interdisciplinary Centre for Clinical Research, Erlangen (A64 to J.H.W.D., J40 to A.R.), the ELAN Fonds of the Universitätsklinikum Erlangen (16-10-05-1 to A.R.), the Career Support Award of Medicine of the Ernst Jung Foundation (to J.H.W.D.), SNF Sinergia CRSII3_154490 (to O.D.), UK-MRC (UI015178805; to A.N.J.M.), the Wellcome Trust (100963/Z/13/Z; to A.N.J.M.) as well as NIH grant AI057459 (to M.H.K.).

References

1. Nathan C, Ding A. Nonresolving inflammation. Cell. 2010; 140:871–882. [PubMed: 20303877]
2. Buckley CD, Gilroy DW, Serhan CN, Stockinger B, Tak PP. The resolution of inflammation. Nat Rev Immunol. 2013; 13:59–66. [PubMed: 23197111]
3. McInnes IB, Schett G. The pathogenesis of rheumatoid arthritis. N Engl J Med. 2011; 365:2205–2219. [PubMed: 22150039]
4. Kotas ME, Medzhitov R. Homeostasis, inflammation, and disease susceptibility. Cell. 2015; 160:816–827. [PubMed: 25723161]
5. Schett G, Gravallese E. Bone erosion in rheumatoid arthritis: mechanisms, diagnosis and treatment. Nature reviews Rheumatology. 2012; 8:656–664. [PubMed: 23007741]
6. Steinman L, Merrill JT, McInnes IB, Peakman M. Optimization of current and future therapy for autoimmune diseases. Nature medicine. 2012; 18:59–65.
7. Schett G, Elewaut D, McInnes IB, Dayer JM, Neurath MF. How cytokine networks fuel inflammation: Toward a cytokine-based disease taxonomy. Nature medicine. 2013; 19:822–824.
8. Serhan CN, Chiang N, Van Dyke TE. Resolving inflammation: dual anti-inflammatory and pro-resolution lipid mediators. Nat Rev Immunol. 2008; 8:349–361. [PubMed: 18437155]
9. Kehoe O, Cartwright A, Askari A, El Haj AJ, Middleton J. Intra-articular injection of mesenchymal stem cells leads to reduced inflammation and cartilage damage in murine antigen-induced arthritis. Journal of translational medicine. 2014; 12:157. [PubMed: 24893776]
10. Brackertz D, Mitchell GF, Mackay IR. Antigen-induced arthritis in mice. I. Induction of arthritis in various strains of mice. Arthritis Rheum. 1977; 20:841–850. [PubMed: 857805]
11. Monach PA, Mathis D, Benoist C. The K/BxN arthritis model. Current protocols in immunology/ edited by John E. Coligan … [et al.]. 2008; Chapter 15(Unit 15):22.

12. Kollias G, et al. Animal models for arthritis: innovative tools for prevention and treatment. Ann Rheum Dis. 2011; 70:1357–1362. [PubMed: 21628308]
13. Ji HB, et al. Cutting edge: the natural ligand for glucocorticoid-induced TNF receptor-related protein abrogates regulatory T cell suppression. J Immunol. 2004; 172:5823–5827. [PubMed: 15128759]
14. Stephens GL, et al. Engagement of glucocorticoid-induced TNFR family-related receptor on effector T cells by its ligand mediates resistance to suppression by CD4+CD25+ T cells. J Immunol. 2004; 173:5008–5020. [PubMed: 15470044]
15. Elyaman W, et al. IL-9 induces differentiation of TH17 cells and enhances function of FoxP3+ natural regulatory T cells. Proc Natl Acad Sci U S A. 2009; 106:12885–12890. [PubMed: 19433802]
16. Gerlach K, et al. TH9 cells that express the transcription factor PU.1 drive T cell-mediated colitis via IL-9 receptor signaling in intestinal epithelial cells. Nat Immunol. 2014; 15:676–686. [PubMed: 24908389]
17. Kaplan MH, Hufford MM, Olson MR. The development and in vivo function of T helper 9 cells. Nat Rev Immunol. 2015; 15:295–307. [PubMed: 25848755]
18. Dardalhon V, et al. IL-4 inhibits TGF-beta-induced Foxp3+ T cells and, together with TGF-beta, generates IL-9+ IL-10+ Foxp3(−) effector T cells. Nat Immunol. 2008; 9:1347–1355. [PubMed: 18997793]
19. Veldhoen M, et al. Transforming growth factor-beta 'reprograms' the differentiation of T helper 2 cells and promotes an interleukin 9-producing subset. Nat Immunol. 2008; 9:1341–1346. [PubMed: 18931678]
20. Ramming A, Druzd D, Leipe J, Schulze-Koops H, Skapenko A. Maturation-related histone modifications in the PU.1 promoter regulate Th9-cell development. Blood. 2012; 119:4665–4674. [PubMed: 22446486]
21. Lu LF, et al. Mast cells are essential intermediaries in regulatory T-cell tolerance. Nature. 2006; 442:997–1002. [PubMed: 16921386]
22. Bannenberg GL, et al. Molecular circuits of resolution: formation and actions of resolvins and protectins. J Immunol. 2005; 174:4345–4355. [PubMed: 15778399]
23. Wilhelm C, et al. An IL-9 fate reporter demonstrates the induction of an innate IL-9 response in lung inflammation. Nat Immunol. 2011; 12:1071–1077. [PubMed: 21983833]
24. Turner JE, et al. IL-9-mediated survival of type 2 innate lymphoid cells promotes damage control in helminth-induced lung inflammation. J Exp Med. 2013; 210:2951–2965. [PubMed: 24249111]
25. Ciccia F, et al. Potential involvement of IL-9 and Th9 cells in the pathogenesis of rheumatoid arthritis. Rheumatology. 2015; 54:2264–72. [PubMed: 26178600]
26. Kundu-Raychaudhuri S, et al. IL-9, a local growth factor for synovial T cells in inflammatory arthritis. Cytokine. 2016; 79:45–51. [PubMed: 26751012]
27. Chang HC, et al. The transcription factor PU.1 is required for the development of IL-9-producing T cells and allergic inflammation. Nat Immunol. 11:527–534.
28. Nowak EC, et al. IL-9 as a mediator of Th17-driven inflammatory disease. J Exp Med. 2009; 206:1653–1660. [PubMed: 19596803]

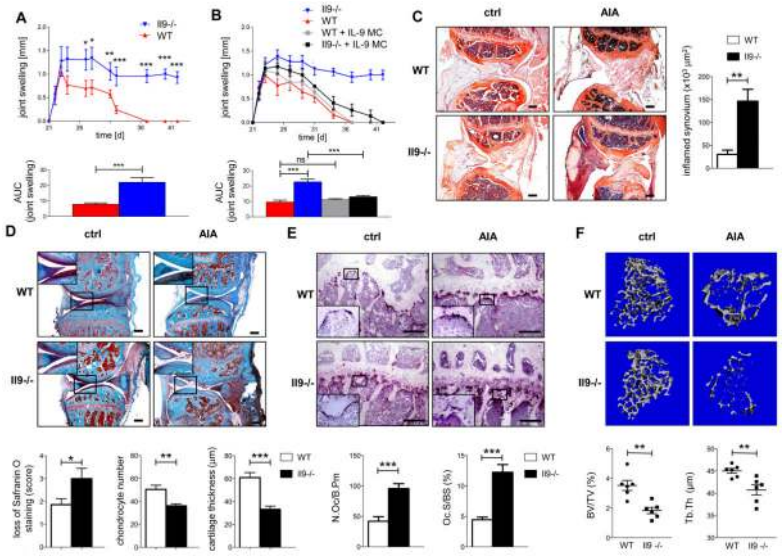

Figure 1. Chronic arthritis in *Il9*-deficient mice

(A, B) Antigen-induced arthritis (AIA) in littermates of **(A)** wild-type (WT) (n=9) and *Il9*$^{-/-}$ mice (n=11) of 3 independent experiments; Y-axis shows knee swelling and the area under the curve (AUC) of knee swelling. **(B)** Overexpression of IL-9 by hydrodynamic gene therapy (HDGT) with mini-circles (MC) encoding for IL-9 in WT (n=7) and *Il9*$^{-/-}$ (n=8) mice at day 22 of AIA. Control mini-circles (ctrl MC) were also injected into WT (n=6) and *Il9*$^{-/-}$ (n=8) mice. **(C, D)** Sections of knee joints from control (ctrl) and AIA-induced mice stained with **(C)** hematoxylin and eosin or **(D)** Safranin-O at day 42 of AIA. Histomorphometric analysis (n>6) of the area of inflammation, proteoglycan loss, chondrocyte number and cartilage thickness. A representative image of each group is included. **(E)** Histomorphometric analysis of osteoclast numbers in the tibia of WT and *Il9*$^{-/-}$ mice (n>6) at day 42 of AIA. A representative image of each group is included. N.Oc/B.Pm, number of osteoclasts per bone parameter; Oc.S/BS, osteoclast surface per bone surface. **(F)** Micro-computed tomography scans and assessment of microarchitectural parameters of tibial bone in ctrl and AIA WT and *Il9*$^{-/-}$ mice (n=6 each) at 14–16 weeks of age. BV/TV, bone volume per total volume. Data are shown as the mean ± SEM. Scale bars correspond to 100 µm. *p<0.05, **p<0.01, ***p<0.001 determined by Student's t test (**a, c–f**) or one-way analysis of variance (ANOVA) with Tukey's *post hoc* test (**a, b**) for experiments including more than 2 groups in one experiment.

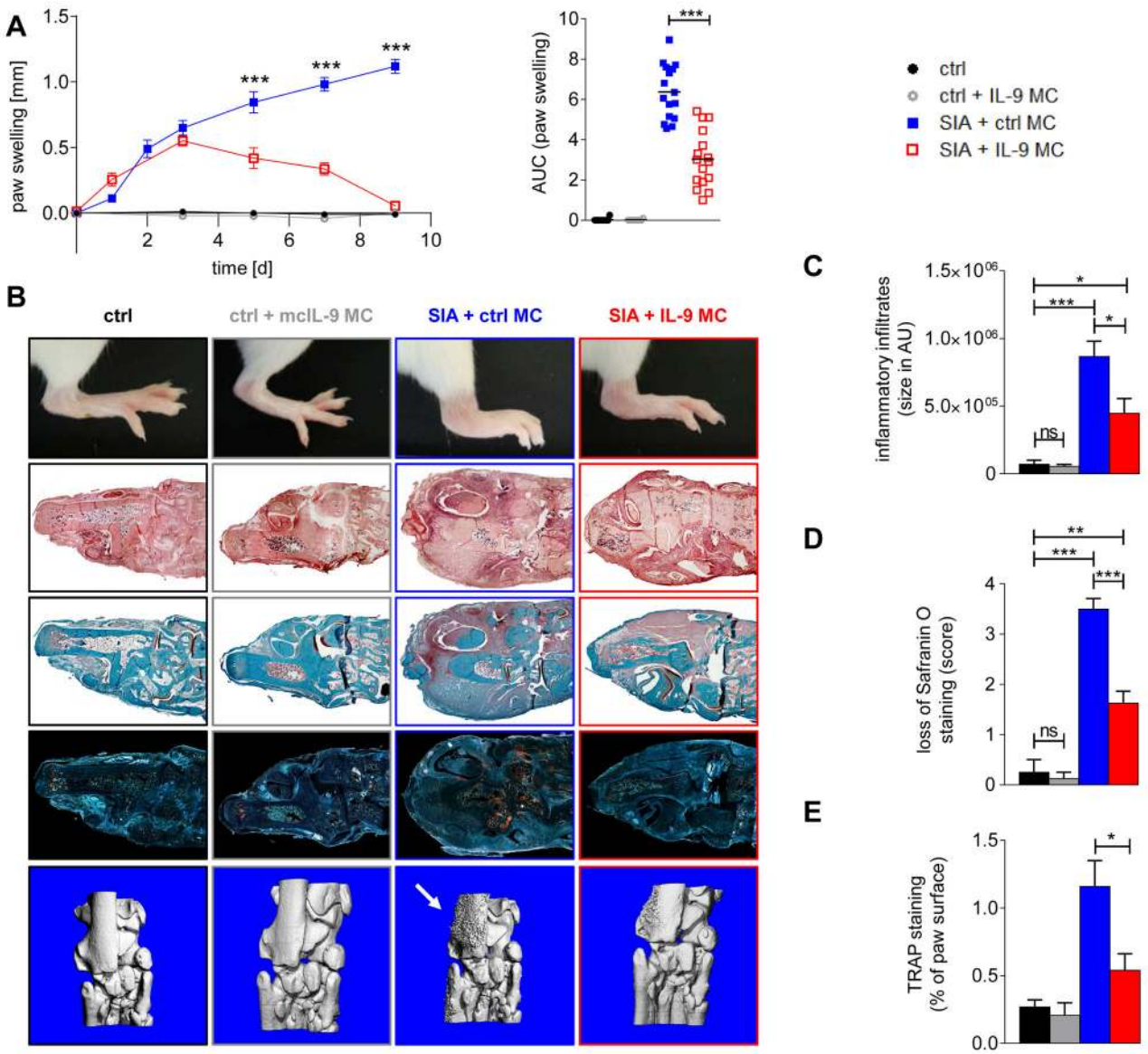

Figure 2. IL-9 accelerates the resolution of arthritis

(A) K/BxN serum induced arthritis (SIA) and non-arthritic mice (ctrl) receiving hydrodynamic gene therapy (HDGT) with mini-circles over-expressing IL-9 (*Il9* MC) (SIA: n=16; ctrl: n=10) or control vector (SIA: n=10; ctrl: n=10). Y-axis shows paw swelling and the area under the curve (AUC) of paw swelling. **(B)** Representative images of paw swelling (line 1), hematoxylin and eosin (H&E) staining of joint tissue (line 2), safranin O staining (line 3), tartrate-resistant acid phosphatase (TRAP) staining (line 4) and micro-computed tomographies (line 5) of the respective groups. **(C)** Quantification of inflammation on H&E stains **(D)** cartilage damage on safranin-O stains and **(E)** bone erosions on TRAP stains. All data are shown as the mean ± SEM. *p<0.05, **p<0.01, ***p<0.001 determined by one-way ANOVA with Tukey's *post hoc* test.

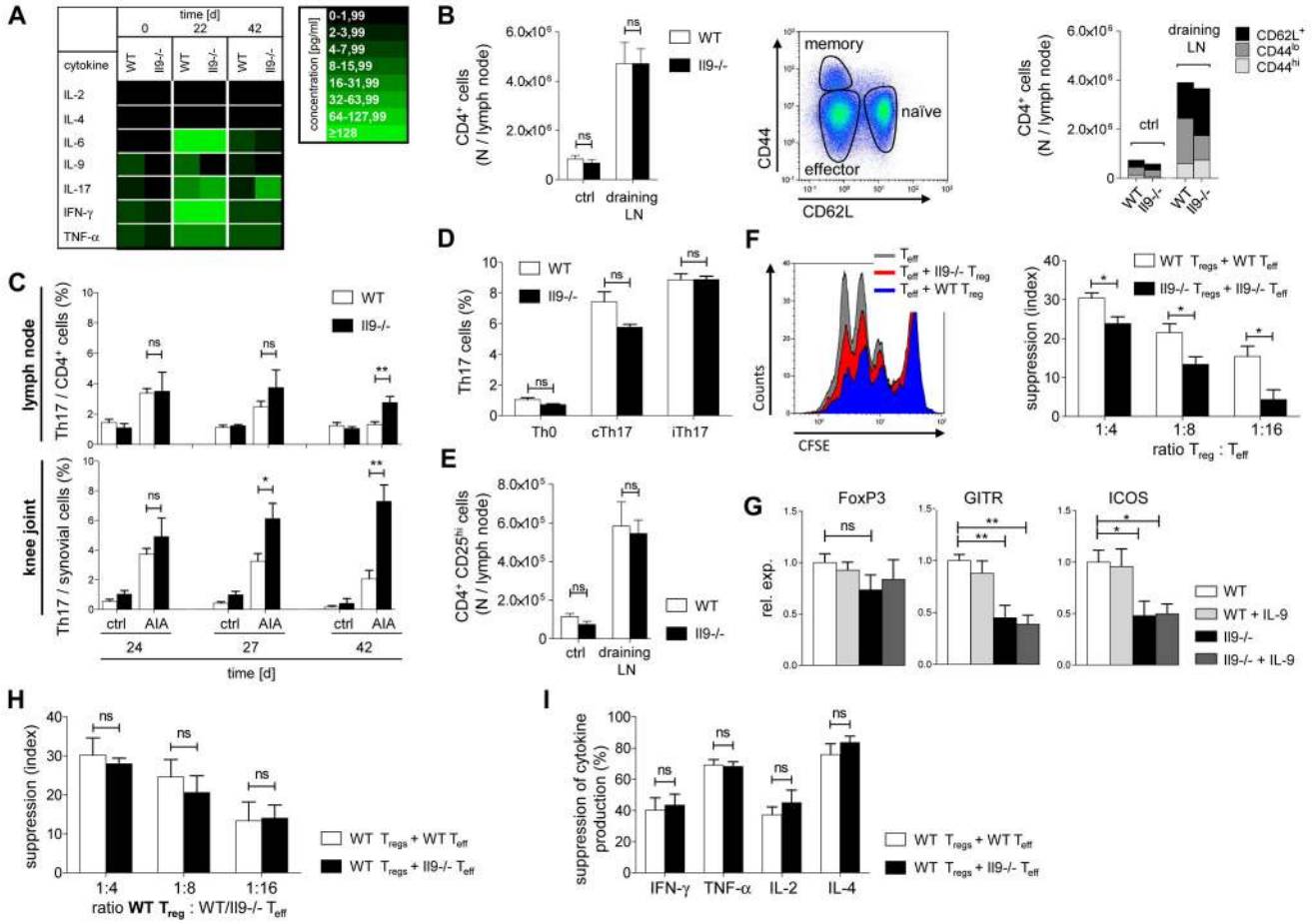

Figure 3. Altered Th17 and Treg responses in arthritic Il9$^{-/-}$ mice

(A) Heat map of serum levels of indicated cytokines from AIA WT (n=9) and *Il9*$^{-/-}$ (n=11) littermates before immunization (d0), after inoculation (d22) and after resolution of inflammation in WT mice (d42). **(B)** CD4^{pos} cell compartment in control (ctrl) and draining lymph nodes (LN) of AIA WT (n=6) and *Il9*$^{-/-}$ (n=6) mice analyzed for memory (CD44^{high}), effector (CD44^{low}) and naïve (CD62L^{pos}) T cells at day 42 of AIA. Representative dot plot is included. **(C)** Th17 cells in ctrl/draining LN, and ctrl/affected knee joint of AIA WT (n=6) and *Il9*$^{-/-}$ (n=6) mice assessed by flow cytometry at day 24, 27 and 42 of AIA. **(D)** Differentiation of CD4+ T cells from WT (n=4) and *Il9*$^{-/-}$ (n=4) mice into conventional (c)Th17 and inflammatory (i)Th17 cells. Th0-stimulating condition served as control. **(E)** Quantification of CD4^{pos}CD25^{pos}FoxP3^{pos} T_{regs} in ctrl and draining LN of AIA WT (n=6) and *Il9*$^{-/-}$ (n=6) mice at day 42 of AIA. **(F)** T_{reg} suppression assay: suppressive capacity of CD4^{pos}CD25^{pos}FoxP3^{pos} T_{regs} from WT (n=7) and *Il9*$^{-/-}$ (n=7) mice. Cell proliferation of CD4^{pos}FoxP3^{neg} responder cells (T_{eff}) was assessed by the dilution of the fluorescent dye CFSE to dividing daughter cells. Representative histograms are included. Suppression was calculated using the division index. **(G)** mRNA expression levels of FoxP3 and co-stimulatory receptors GITR and ICOS on sorted CD4^{pos}CD25^{high}FoxP3^{pos} T_{regs} (n=8 each) stimulated with anti-CD3/28 in the presence and absence of recombinant IL-9 for 48h. **(H)** T_{reg} suppression assay: susceptibility of WT and *Il9*$^{-/-}$ (n=6 each) T_{eff} to become

suppressed by WT T_{regs}. **(I)** WT T_{reg}-induced suppression of cytokines released from WT and *Il9*$^{-/-}$ T_{effs} (n=6 each). All data are shown as the mean ± SEM of 3–6 independent experiments of each group. *p<0.05, **p<0.01, ***p<0.001 determined by Student's t test (**b, e**) or ordinary one-way ANOVA with Tukey's *post hoc* test (**c, d, f–i**).

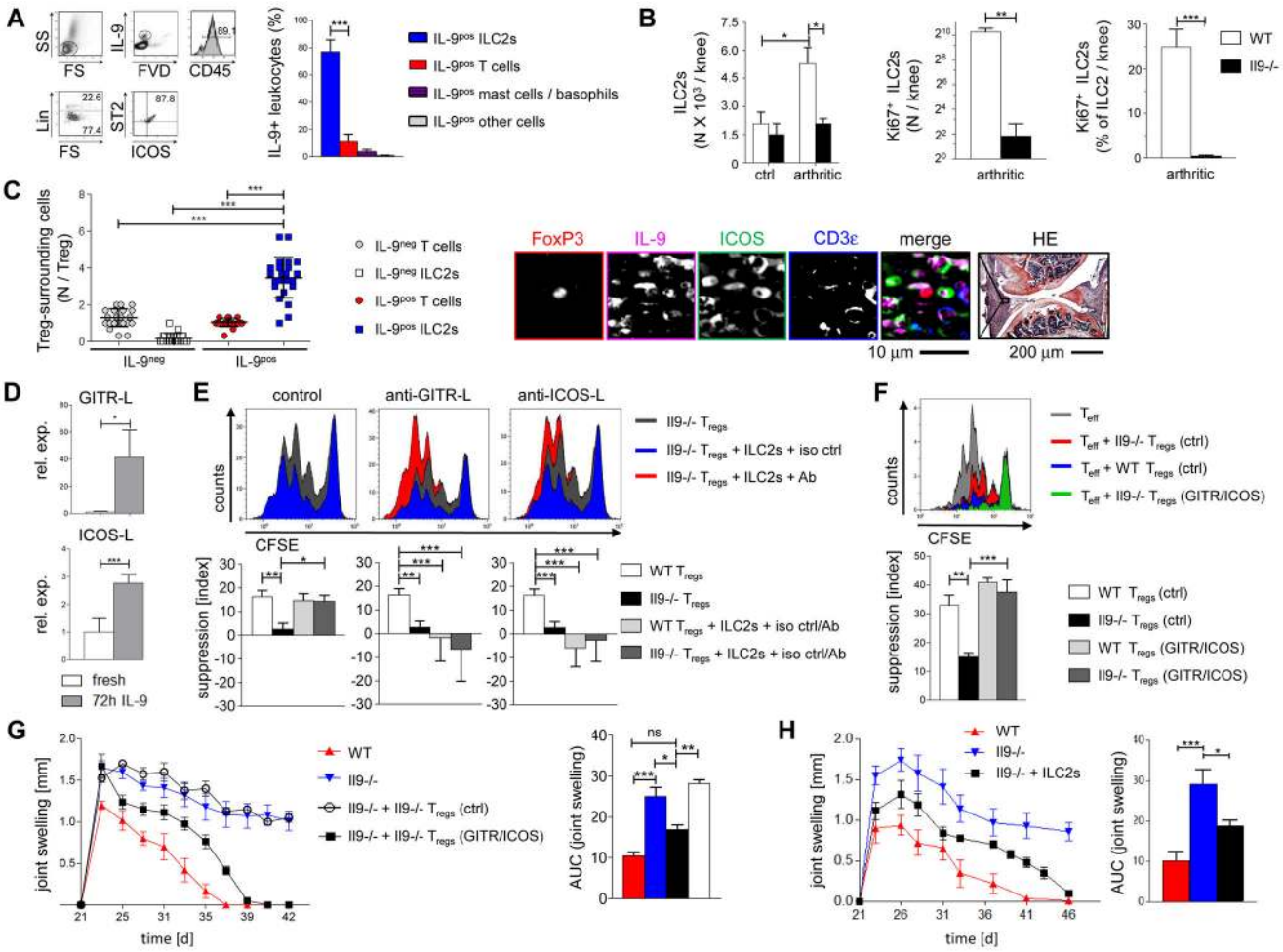

Figure 4. ILC2s sustain suppressive capacity of T_{regs} by co-stimulation via ICOS-L/ICOS and GITR-L/GITR

(A) Flow cytometric analysis of AIA in *Il9*^{citrine} reporter mice (n=7). Cells isolated from joints at day 27 were stratified due to viability, IL-9, CD45, expression of lineage markers (Lin; CD3ε, CD11b, CD11c, CD45R, CD49b, FcER1a, Gr-1, TER-119), ICOS, and ST2. Representative plots are shown. **(B)** Quantification of ILC2s in ctrl and arthritic joints from AIA WT and *Il9*$^{-/-}$ mice at day 27 (n=5 each) by flow cytometry. Ki67 was co-stained to assess proliferation of ILC2s. **(C)** IF microscopy of inflamed joints of WT mice (n=5) with AIA at day 27 stained for Foxp3, IL-9, ICOS and CD3ε. Randomly chosen T_{regs} from 5 tissue sections per mouse were analyzed for surrounding cells stratified by IL-9 production and surface markers. Data are shown as mean ± SEM. Representative images are shown. (**D**) mRNA expression levels of GITRL and ICOSL in sorted ILC2s cultured in the presence and absence of recombinant IL-9 for 72h (n=5 each). **(E–G)** T_{reg} suppression assay; suppressive capacity of CD4^{pos}FoxP3^{pos} T_{regs} from WT and *Il9*$^{-/-}$ mice: **(E)** co-cultures w/o ILC2s in the presence/absence of blocking antibodies (Ab) against GITRL or ICOSL (n>5 each). **(F)** Pre-stimulation of *Il9*$^{-/-}$ T_{regs} with recombinant ICOSL and agonistic anti-GITR before co-culture with responder cells (T_{eff}; n>5 each); isotype control (iso ctrl) antibody was used as control. Representative histograms are included. Suppression was calculated using the

division index. Data are shown as the mean ± SEM of 3 independent experiments of each group. **(G)** *Il9*$^{-/-}$ T_{regs} were pre-stimulated *ex vivo* with recombinant ICOSL and agonistic anti-GITR before adoptive transfer into *Il9*$^{-/-}$ mice induced for AIA (n=5 each). **(H)** ILC2s were adoptively transferred into *Il9*$^{-/-}$ mice induced for AIA (n=5 each). Y-axis shows knee swelling and the area under the curve (AUC) of knee swelling. All data are shown as the mean ± SEM of 3 independent experiments of each group. *p<0.05, **p<0.01, ***p<0.001 determined by one-way ANOVA with Tukey's *post hoc* test (**a–c, e–h**) or Student's t test (**b, d**).

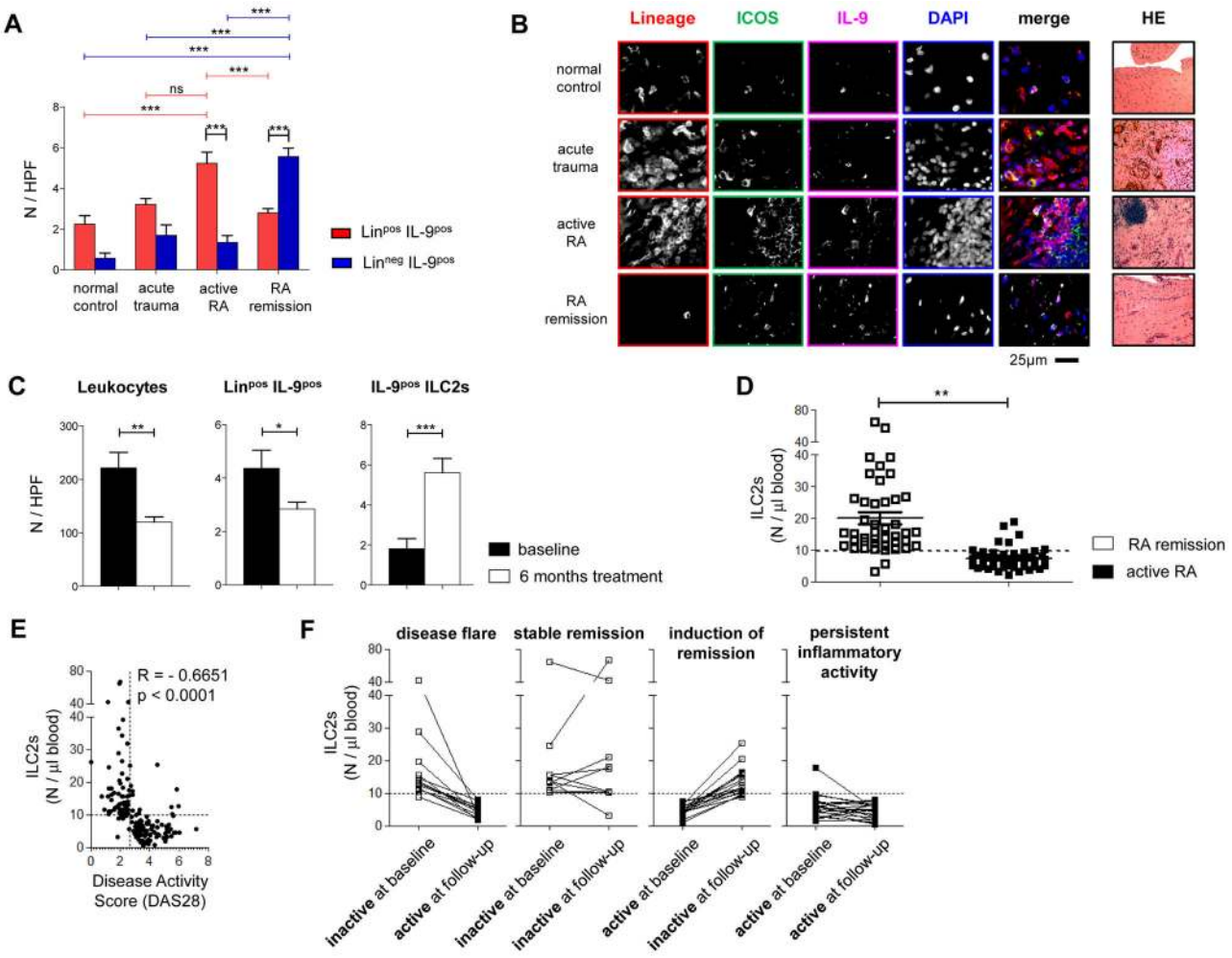

Figure 5. IL-9 during resolution of human arthritis

(A–C) IF microscopy of human synovial biopsies stained for lineage markers (Lin; CD3, CD11b, CD16, mast cell tryptase), ICOS, IL-9 and DAPI. **(A)** Histomorphometric analysis was performed by quantification of Lin^{pos}, Lin^{pos}/IL-9^{pos} and Lin^{neg}/$ICOS^{pos}$/IL-9^{pos} (ILC2) cells per 0.3 mm^2 of synovial tissue by five independent and blinded researchers. Data are shown as the mean ± SEM. Included are normal controls (n=11), patients with acute trauma (n=8), rheumatoid arthritis (RA) patients with active disease (n=19; DAS28 score >3.2) and RA patients in remission (n=19; DAS28 score <2.6). **(B)** Representative IF images; **(C)** Quantification of Lin^{pos}, Lin^{pos}/IL-9^{pos} and Lin^{neg}/$ICOS^{pos}$/IL-9^{pos} (ILC2) cells in RA patients with high disease activity (DAS28: 5.1 ± 1.2; n=10) before and after 6 months of treatment with anti-rheumatic drugs inducing disease remission. **(D–F)** Absolute counts of ILC2s in the blood of RA patients (n=111); **(D)** ILC2 counts in patients with active disease (DAS28 ≥3.2; n=61) and inactive disease (DAS28<2.6; n=50); data are shown as the mean ± SEM. **(E)** Correlation between ILC2 counts and disease activity score (DAS28); the correlation analysis used was nonparametric (Spearman's correlation). **(F)** Longitudinal observation of ILC2 counts at baseline and 6–12 month follow-up in RA patients (n=63) stratified into 4 groups according to baseline and follow-up disease activity (inactive vs.

active). *p<0.05, **p<0.01, ***p<0.001 determined by one-way ANOVA with Tukey's *post hoc* test (**a**) or Student's t test (**c,** d).